

# FIRST DETECTION OF <sup>56</sup>CO GAMMA-RAY LINES FROM TYPE IA SUPERNOVA (SN2014J) WITH INTEGRAL.

E. CHURAZOV<sup>1,2</sup>, R. SUNYAEV<sup>1,2</sup>, J. ISERN<sup>3</sup>, J. KNÖDLSIEDER<sup>4,5</sup>, P. JEAN<sup>4,5</sup>, F. LEBRUN<sup>6</sup>, N. CHUGAI<sup>7</sup>, S. GREBENEV<sup>1</sup>,  
E. BRAVO<sup>8</sup>, S. SAZONOV<sup>1,9</sup>, M. RENAUD<sup>10</sup>

<sup>1</sup>Space Research Institute (IKI), Profsovnaya 84/32, Moscow 117997, Russia

<sup>2</sup>Max Planck Institute for Astrophysics, Karl-Schwarzschild-Strasse 1, 85741 Garching, Germany

<sup>3</sup>Institut for Space Sciences (ICE-CSIC/IEEC), 08193 Bellaterra, Spain

<sup>4</sup>Université de Toulouse; UPS-OMP; IRAP; Toulouse, France

<sup>5</sup>CNRS; IRAP; 9 Av. colonel Roche, BP 44346, F-31028 Toulouse cedex 4, France

<sup>6</sup>APC, Univ Paris Diderot, CNRS/IN2P3, CEA/Irfu, Obs de Paris, Sorbonne Paris Cité, France

<sup>7</sup>Institute of Astronomy of the Russian Academy of Sciences, 48 Pyatnitskaya St. 119017, Moscow, Russia

<sup>8</sup>E.T.S.A.V., Univ. Politecnica de Catalunya, Carrer Pere Serra 1-15, 08173 Sant Cugat del Valles, Spain

<sup>9</sup>Moscow Institute of Physics and Technology, Institutsky per. 9, 141700 Dolgoprudny, Russia and

<sup>10</sup>LUPM, Université Montpellier 2, CNRS/IN2P3, CC 72, Place Eugène Bataillon, F-34095 Montpellier Cedex 5, France

*Draft version May 15, 2014*

## ABSTRACT

We report the first ever detection of <sup>56</sup>Co lines at 847 and 1237 keV and a continuum in the 200-400 keV band from the Type Ia supernova SN2014J in M82 with *INTEGRAL* observatory. The data were taken between 50th and 100th day since the SN2014J outburst. The line fluxes suggest that  $0.62 \pm 0.13 M_{\odot}$  of radioactive <sup>56</sup>Ni were synthesized during the explosion. Line broadening gives a characteristic ejecta expansion velocity  $V_e \sim 2100 \pm 500 \text{ km s}^{-1}$ . The flux at lower energies (200-400 keV) flux is consistent with the three-photon positronium annihilation, Compton downscattering and absorption in the  $\sim 1.4 M_{\odot}$  ejecta composed from equal fractions of iron-group and intermediate-mass elements and a kinetic energy  $E_k \sim 1.4 \cdot 10^{51} \text{ erg}$ . All these parameters are in broad agreement with a “canonical” model of an explosion of a Chandrasekhar-mass White Dwarf (WD), providing an unambiguous proof of the nature of Type Ia supernovae as a thermonuclear explosion of a solar mass compact object.

## 1. INTRODUCTION

A Type Ia supernova is believed to be a thermonuclear explosion of a carbon-oxygen white dwarf (WD) with a mass not far from a Chandrasekhar limit (see, e.g., Nomoto et al. 1984; Woosley & Weaver 1986; Hillebrandt & Niemeyer 2000). Plausible scenarios include accretion-driven mechanisms or a merger of two white dwarfs. The detailed physics of the explosion (e.g., deflagration or detonation) and the evolutionary path of a compact object towards the explosion remain a matter of debate (Gilfanov & Bogdán 2010; Röpke et al. 2012; Malone et al. 2014; Moll et al. 2014) although the WD merger scenario becoming prevalent. Apart from the interest in the physics specific to type Ia supernova, these objects serve as a “standard candle” in Cosmology (Riess et al. 1998; Perlmutter et al. 1999), since their peak luminosity can be predicted from the properties of the optical light curves. These light curves are best modeled as reprocessing of the energy released by the decay chain of the radioactive  $^{56}\text{Ni} \rightarrow ^{56}\text{Co} \rightarrow ^{56}\text{Fe}$  in the form of gamma-ray photons, positrons and kinetic energy of electrons. Due to Compton scattering during first 10-20 days the ejecta are opaque for gamma-ray lines produced in the bulk of the ejecta. At later times the ejecta become progressively more transparent and a large fraction of gamma-rays escape the ejecta. This leads to a robust prediction of a gamma-ray emission from SN Ia after few tens of days, dominated by the gamma-ray lines of <sup>56</sup>Co, which, however, were never detected. The downscattered hard X-ray continuum from SN1987A in LMC (nearest Type II supernova in recent history) was discovered in the 25-

300 keV band (Sunyaev et al. 1987) using HEXE and PULSAR X-1 detectors of MIR/KVANT Space Station. Gamma-ray lines of Co from SN1987A were detected several months later (Matz et al. 1988). Early appearance of hard X-ray emission from SN1987A clearly demonstrated that Co is mixed over ejecta (see, e.g., Sunyaev et al. 1990).

SN2014J in M82 was discovered on Jan. 21, 2014 by S.J.Foosey team. The reconstructed (Zheng et al. 2014) date of the explosion is Jan. 14.75 UT. At the distance of M82 ( $D \sim 3.5 \text{ Mpc}$ , Karachentsev & Kashibadze 2006) this is the nearest SN Ia in several decades. Another recent SNIa SN2011fe was too far ( $D \sim 6.4 \text{ Mpc}$ ) to result in a detectable gamma-ray emission, yielding an upper-limit on the <sup>56</sup>Co line flux from the INTEGRAL observation (Isern et al. 2013). The proximity of the SN2014J triggered many follow-up observations, including those by *INTEGRAL* (Kuulkers 2014). *INTEGRAL* started observing SN2014J on 2014 Jan. 31 and ended on 2014 Apr. 24. Here we report the detection of <sup>56</sup>Co lines at 847 and 1238 keV<sup>1</sup> and Compton down-scattered and orthopositronium continua by INTEGRAL 50-100 days after the explosion.

## 2. DATA AND ANALYSIS

*INTEGRAL* is an ESA scientific mission dedicated to fine spectroscopy and imaging of celestial  $\gamma$ -ray sources in the energy range 15 keV to 10 MeV.

<sup>1</sup> The evidence for the 847 keV line in the first portion of the considered data set was reported by us in Churazov et al. (2014), see also Isern et al. (2014)

The *INTEGRAL* data used here were accumulated during revolutions 1391-1407<sup>2</sup>, corresponding to the period  $\sim 50$ -100 days after the explosion (proposals: 1170002/PI:Sunyaev, 1140011/PI:Isern, 1170001/public). Periods of very high and variable background due to solar flares were omitted from the analysis. Total exposure of the clean data set is  $\sim 2.6$  Ms.

### 2.1. SPI data analysis

SPI is a coded mask germanium spectrometer on board *INTEGRAL*. The instrument consists of 19 individual Ge detectors, has a field of view of  $\sim 30^\circ$  (at zero response), an effective area  $\sim 70$  cm<sup>2</sup> at 0.5 MeV and energy resolution of  $\sim 2$  keV (Vedrenne et al. 2003). Effective angular resolution of SPI is  $\sim 2^\circ$ . During SN2014J observations 15 out of 19 detectors were operating, resulting in slightly reduced sensitivity and imaging capabilities compared to initial configuration. The data analysis follows the scheme implemented in Churazov et al. (2005, 2011, see §4.1 for details).

The spectrum derived from entire data set at energies above 400 keV is shown in Fig.1 with red points. Black curve shows a fiducial model (see §3.1) of the supernova spectrum for day 75 after the explosion. The model spectrum is binned similarly to the SN spectrum. The signatures of the 847 and 1237 keV lines are clearly seen in the spectrum (and tracers of weaker lines at 511 and 1038 keV). Low energy (below 400 keV) part of the spectrum is not shown because of possible contamination of the spectrum by off-diagonal response of SPI related to the flux of bright <sup>56</sup>Co lines at higher energies. At these energies we use ISGRI/IBIS data instead (see §2.2).

By varying the assumed position of the source we construct  $40^\circ \times 40^\circ$  image of signal-to-noise ratio in the 800-880 and 1200-1300 keV energy bands (Fig.2). SN2014J is detected at 3.9 and 4.3  $\sigma$  in these two bands respectively. These are the highest peaks in both images.

### 2.2. ISGRI/IBIS data analysis

The primary imaging instrument onboard *INTEGRAL* is IBIS (Ubertini et al. 2003) – a coded-mask aperture telescope with the CdTe-based detector ISGRI (Lebrun et al. 2003). It has higher sensitivity for continuum emission than SPI in the 20–300 keV range and has a spatial resolution  $\sim 12'$ . The energy resolution of ISGRI is  $\sim 10\%$  at 100 keV.

The image (see §4.2) obtained by ISGRI during SN2014J late observations in 100-600 keV energy band is shown in the left panel of Fig.3. For comparison, the right panel shows the same field observed during M82 observations in October-December 2013, i.e. a few months before the SN2014J outburst (*INTEGRAL* proposal 1020008, PI: S. Sazonov). The inspection of lower energy images in the 25-50 keV band shows that images taken in 2013 and 2014 are similar, while at higher energies (above 100 keV) there is an excess at the position of SN2014J only in the 2014 data<sup>3</sup> Previous ISGRI observations of this field in 2009-2012, with a total exposure of

about 6 Msec, revealed no significant signal at energies above 50 keV from the M82 galaxy (Sazonov et al. 2014).

## 3. DISCUSSION

Despite of its proximity the SN2014J is still an extremely faint source in gamma-rays. The flux from the source contributes only a fraction of a percent to the SPI count rate on top of the time-variable (by tens of %) detector background. While precise measurements of line fluxes are challenging, a combination of spectral and imaging information makes our results very robust, although some systematic uncertainties of order  $\sim 30\%$  should still be allowed for.

The results described in the previous section can be summarized as follows: (i) *INTEGRAL* detects significant emission from two brightest gamma-ray lines associated with <sup>56</sup>Co decay, (ii) the lines are significantly broadened, (iii) low energy (<400 keV) emission is present. We now discuss the most basic implications of these results.

### 3.1. Fiducial model

While detailed modeling of SN2014J properties is beyond the scope of this Letter, we use a simple reference model to qualitatively compare our results with expected gamma-ray emission from a “canonical” Type Ia supernova (see also The & Burrows (2014) for detailed predictions for a set of commonly used models). Our reference model assumes that the total mass of the ejecta is  $M = 1.38 M_\odot$ , the kinetic energy of the explosion is  $E_K = 1.3 \cdot 10^{51}$  erg, the initial mass of <sup>56</sup>Ni is  $M_{Ni} = 0.7 M_\odot$  and half of the total ejecta mass is composed from iron-group elements. We ignore possible anisotropy of the <sup>56</sup>Ni distribution expected in the scenario of WD mergers (Moll et al. 2014). The density of the homologously expanding ejecta follows the exponential law  $\rho \propto e^{-v/V_e}$  (e.g., Dwarkadas & Chevalier 1998;

Woosley et al. 2007), where  $V_e = \sqrt{\frac{E_K}{6M}} \sim 2800$  km s<sup>-1</sup> and is truncated at  $v = 10 V_e$ . All elements are uniformly mixed through the entire ejecta. The Monte-Carlo radiative transfer code is used to calculate emergent spectrum, which includes full treatment of the Compton scattering (coherent and incoherent) and photoabsorption. Pair production by gamma-ray photons is neglected. The positrons produced by  $\beta^+$  decay of <sup>56</sup>Co (19% of all decays) annihilate in place via positronium formation and both two-photon annihilation and ortho-positronium continuum are included. Our reference model was calculated for 75th day since the explosion. A time delay due to finite propagation time of the photons is neglected (it amounts to few days from the radius where the bulk of the mass is located).

### 3.2. <sup>56</sup>Ni mass and energy deposition rate

The best-fitting parameters of two gamma-ray lines are given in Table 1. Since the decay time of <sup>56</sup>Co  $\tau = 111.4$  days and branching ratios (1 and 0.66 for 847 and 1238 keV lines respectively) are known, it is straightforward to convert line fluxes into the mass or <sup>56</sup>Co, visible to *INTEGRAL* at the time of observation (see Table 1). This value  $M_{Co} \sim 0.2 M_\odot$  can be considered as a model independent lower limit on the amount

<sup>2</sup> <http://integral.esac.esa.int/isocweb/schedule.html?action=intro>

<sup>3</sup> Neither ISGRI, nor SPI can distinguish the emission of SN2014J from the emission of any other source in M82. ISGRI however can easily differentiate between M82 and M81 separated by  $\sim 30'$ .

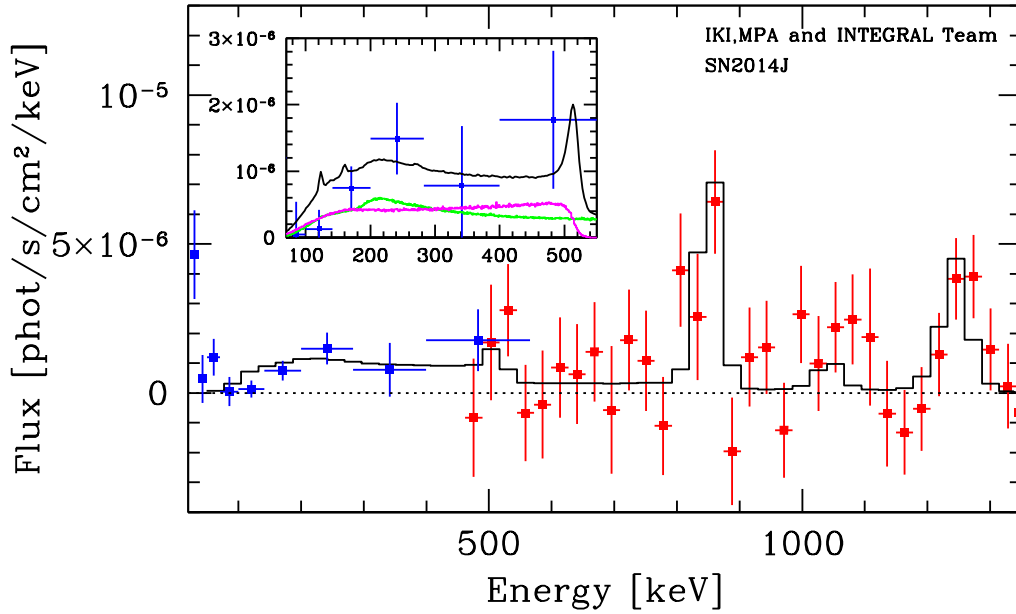


FIG. 1.— Spectrum of the SN2014J obtained by SPI over the period  $\sim 50 - 100$  days after the outburst (red). Blue points show ISGRI/IBIS data for the same period. The flux below  $\sim 60$  keV is dominated by the emission of M82 itself (as seen in 2013 during M82 observations with INTEGRAL). Black curve shows a fiducial model of the supernova spectrum for day 75 after the explosion. For the sake of clarity the inset shows the lower energy part of the spectrum. The expected contributions of three-photon positronium annihilation (magenta) and Compton-downscattered emission from 847 and 1238 keV lines (green) are shown in the inset.

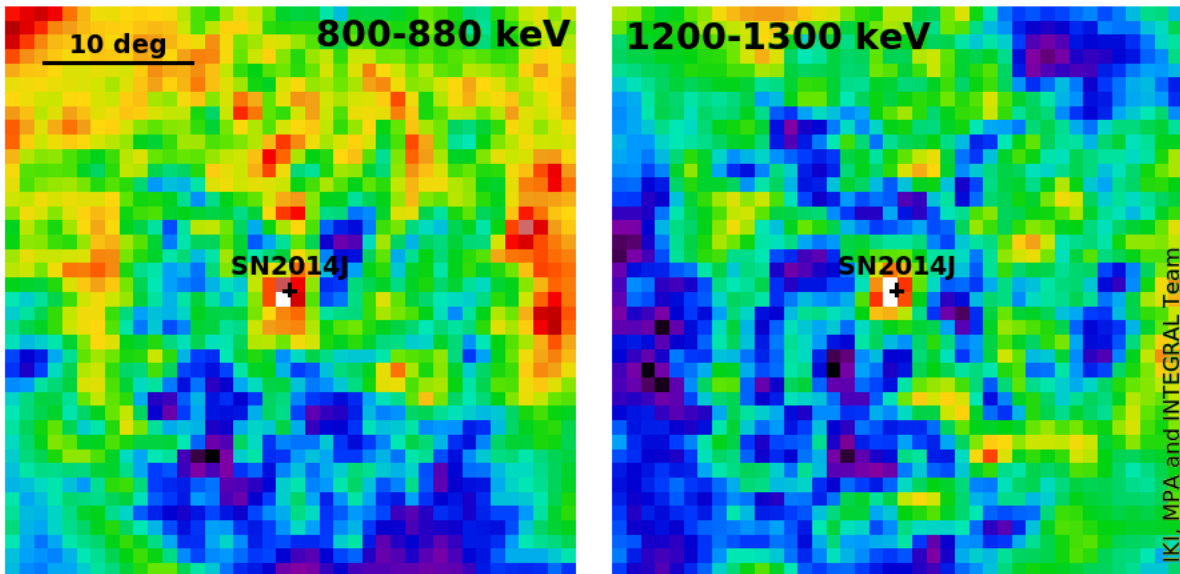


FIG. 2.— Signatures of  $^{56}\text{Co}$  lines at 847 and 1238 keV in SPI images. Broad bands 800-880 keV and 1200-1300 keV are expected to contain the flux from these lines with account for expected broadening (and shift) due to the ejecta expansion and opacity effects. The source is detected at  $3.9$  and  $4.3 \sigma$  in these two bands.

TABLE 1  
PARAMETERS<sup>a</sup> OF THE OBSERVED SPECTRUM AND THE REFERENCE MODEL

Parameter	847 keV line	1238 keV line	Mean	200-400 keV
Flux, $10^{-4}$ phot cm $^{-2}$ s $^{-1}$	$2.34 \pm 0.74$	$2.78 \pm 0.74$	...	$2.0 \pm 0.78$
Model	3.48	2.53	...	2.1
Luminosity, $10^{41}$ erg s $^{-1}$	4.7	8.1	...	1.4
$^{56}\text{Co}$ Mass, $M_{\odot}$ (“Directly visible”)	$0.16 \pm 0.05$	$0.27 \pm 0.07$	...	...
$^{56}\text{Co}$ Mass, $M_{\odot}$ (“Corrected for escape”)	$0.26 \pm 0.08$	$0.42 \pm 0.11$	$0.34 \pm 0.068$	...
$^{56}\text{Ni}$ Mass, $M_{\odot}$	$0.47 \pm 0.15$	$0.77 \pm 0.2$	$0.62 \pm 0.13$	...
Model	...	...	0.70	...
$V_{shift}$ (l.o.s. velocity), km s $^{-1}$	$-1900 \pm 1600$	$-4300 \pm 1600$	$-3100 \pm 1100$	...
Model	-1370	-1190	-1280	...
Line width (l.o.s. velocity rms) $\sigma_{\gamma}$ , km s $^{-1}$	$3600 \pm 1300$	$4700 \pm 1400$	$4100 \pm 960$	...
Model	5890	5830	5860	...
$V_e$ , km s $^{-1}$	$1800 \pm 630$	$2400 \pm 715$	$2100 \pm 500$	...
Model	...	...	2810	...

NOTE. — <sup>a</sup> - pure statistical errors (a systematic error of  $\sim 30\%$  should be allowed for)

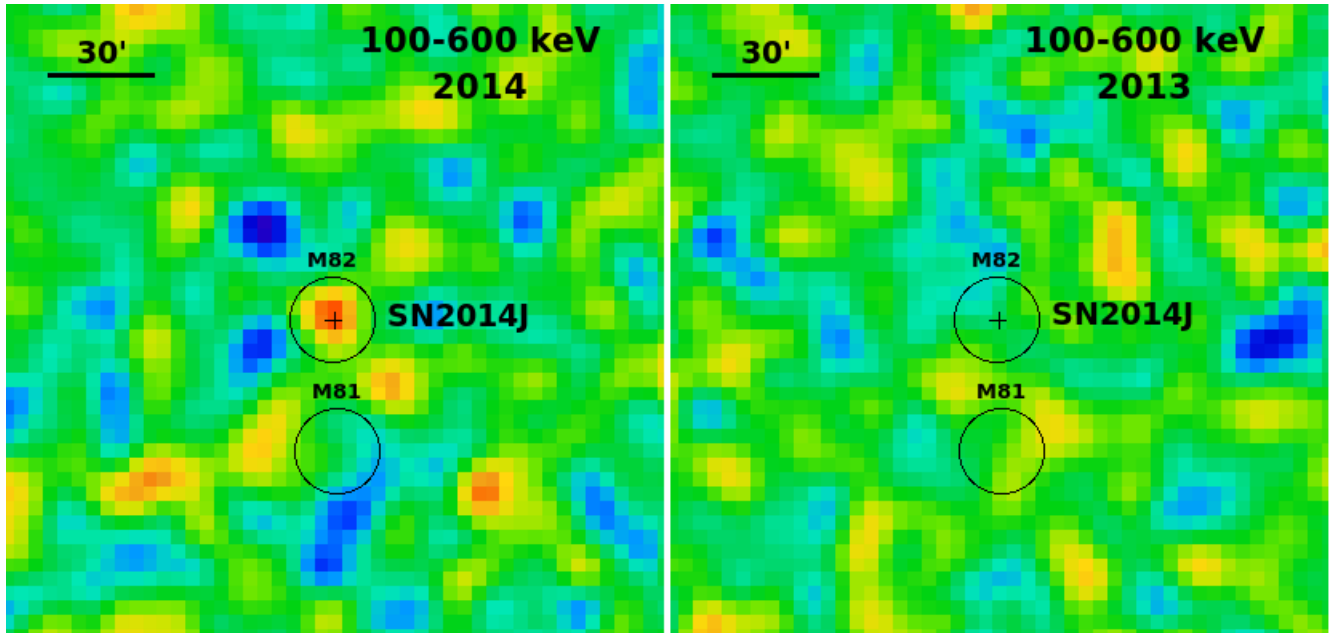


FIG. 3.— ISGRI images of the M82 field in the 100-600 keV band in 2014 (left) and 2013 (rights). A source at  $\sim 3.7\sigma$  is present at the position of SN2014J.

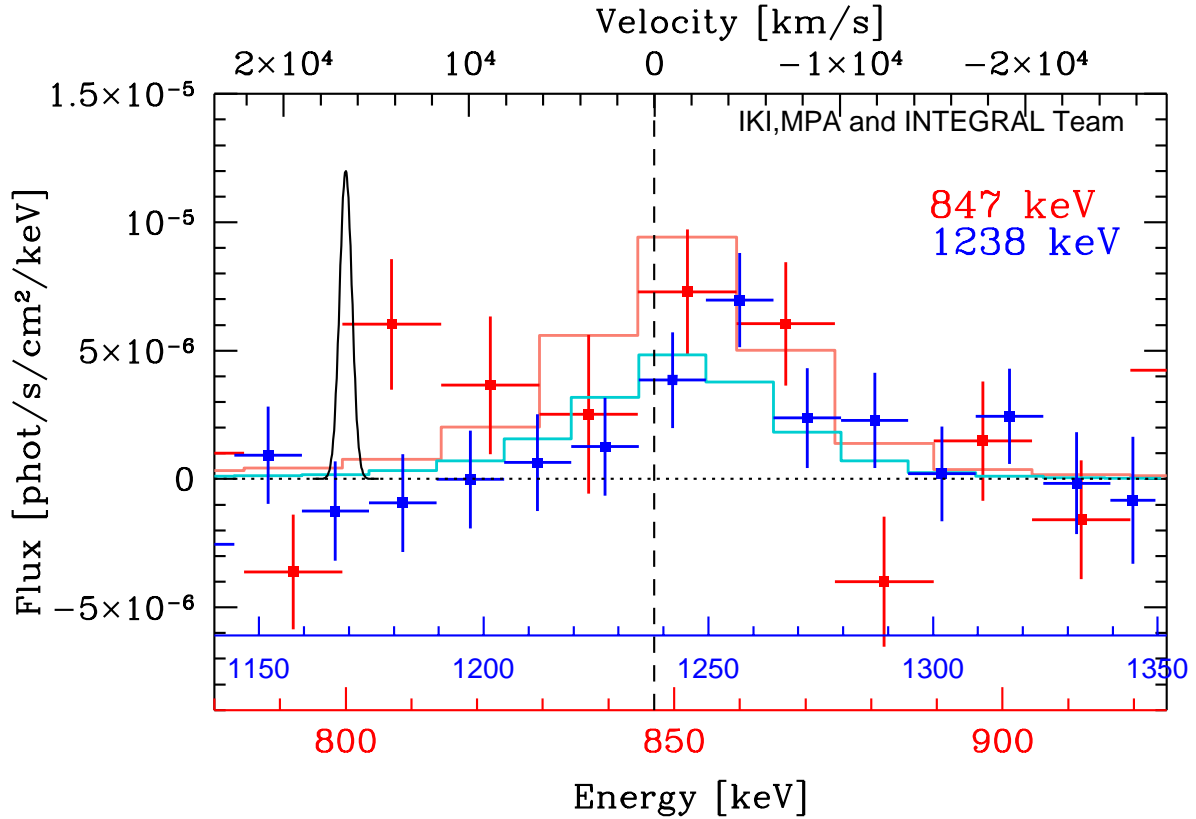


FIG. 4.— Broadening of the 847 and 1238 keV lines. Red points show the SPI spectrum in the 720-920 keV range. Red histogram shows the line profile in the fiducial model. The blue points show the SPI spectrum of the 1238 keV line. For comparison a Gaussian line at 800 keV with the width, corresponding to the SPI intrinsic energy resolution is shown with a black line. Both observed lines are clearly broadened. Upper axis shows the velocity needed to shift the line to a given energy.

of  $^{56}\text{Co}$  (or equivalently a lower limit on the initial  $^{56}\text{Ni}$  mass  $M_{Ni} = 0.36 M_{\odot}$ ). The fraction of line photons escaping the ejecta without interactions was estimated from the model: 0.60 (847 KeV) and 0.64 (1238 keV). These values were used to correct observed fluxes to derive an estimate of the  $^{56}\text{Co}$  mass  $M_{Co} = 0.34 \pm 0.07 M_{\odot}$  at day 75. Finally a correction factor of  $1/0.55$  has been applied to convert the mass of  $^{56}\text{Co}$  at day 75 to the initial mass of  $^{56}\text{Ni}$ :  $M_{Ni} = 0.62 \pm 0.13 M_{\odot}$  (see Table 1).

The same data can be used to estimate total energy deposition rate in the SN2014J during INTEGRAL observations. Total energy released during decay of  $^{56}\text{Co}$  isotope (Nadyozhin 1994) is split between neutrinos ( $\sim 0.8$  MeV), kinetic energy of positrons ( $\sim 0.12$  MeV) and gamma-rays ( $\sim 3.6$  MeV). In our fiducial model  $f \sim 77\%$  of the luminosity in gamma-rays escapes the ejecta. Remaining fraction  $(1 - f) = 23\%$  is deposited in the ejecta (ignoring bremsstrahlung radiation by electrons). Adding kinetic energy of positrons and 23% of the gamma-ray luminosity produced by  $0.34 M_{\odot}$  of  $^{56}\text{Co}$  at day 75 yields an estimate of the energy deposition rate in the ejecta  $\sim 1.1 \cdot 10^{42}$  erg  $s^{-1}$ , while  $\sim 3.3 \cdot 10^{42}$  erg  $s^{-1}$  escape the ejecta in the form of hard X-rays and gamma-rays.

### 3.3. $^{56}\text{Ni}$ mass from optical data

The independent estimate of the  $^{56}\text{Ni}$  mass can be obtained from the bolometric light curve. We use the ap-

proach prompted by Arnett (1982) who found that the bolometric luminosity at the maximum is equal to the power of the radioactive decay at this moment. In the case of SN 2014J the maximum bolometric luminosity is  $1.13 \times 10^{43}$  erg  $s^{-1}$  and it is attained on day 17.7 after the explosion (Margutti et al. 2014). This implies the  $^{56}\text{Ni}$  mass of  $0.37 M_{\odot}$ . Note that Margutti et al. (2014) adopt absorption  $A_V = 1.7$  mag whereas Goobar et al. (2014) infers the larger absorption,  $A_V = 2.5$  mag. The latter implies the  $^{56}\text{Ni}$  mass of  $0.77 M_{\odot}$ . The bolometric luminosity thus suggests that the  $^{56}\text{Ni}$  mass of SN 2014J lies the range of  $0.57 \pm 0.2 M_{\odot}$ . These values agree with the estimates based on gamma-lines. The uncertainty of the distance ( $D = 3.53 \pm 0.26$  Mpc, Karachentsev & Kashibadze 2006) corresponds to the additional uncertainty in mass  $\sim 0.08 M_{\odot}$ . Similar uncertainty applies to gamma-ray data.

### 3.4. Ejecta expansion and the total ejecta mass

In a fully transparent ejecta the centroid of emerging gamma-ray lines should be unshifted (at least to the first order in  $V_e/c$ , where  $c$  is the speed of light). Opacity suppresses gamma-rays coming from the receding part of the ejecta, leading to a blue shift of the visible line. Blue shift is indeed observed for both lines, when fitting their profiles with a Gaussian (see Table 1 and Fig. 4). Corresponding mean velocity is  $V_{shift} = -3100 \pm 1100$  km  $s^{-1}$  is slightly higher (by  $1.7\sigma$ )

than the expected shift  $V_{shift,mod} \sim -1280 \text{ km s}^{-1}$  estimated from the model for gamma-ray photons escaping the ejecta without interactions.

The expected line broadening (rms of the line-of-sight (l.o.s) velocity)  $\sigma_\gamma$  for transparent ejecta is directly related to the characteristic expansion velocity  $\sigma_\gamma = 2V_e$ . Indeed, in the model we found for directly escaping photons  $\sigma_\gamma = 5860 \text{ km s}^{-1} \sim 2.1 V_e$ . The Gaussian fit to the observed lines yields  $\sigma_\gamma = 4100 \pm 960 \text{ km s}^{-1}$  and provides an estimate of  $V_e = 2100 \pm 500 \text{ km s}^{-1}$ .

Finally, at lower energies (100-400 keV) the emerging flux is dominated by Compton scattering of 847 and 1238 keV photons and the ortho-positronium continuum from positrons annihilation (see inset in Fig. 1). The strength of the signal in this band depends on the intensity of the gamma-ray lines ( $M_{Ni}$ ), on the Thomson depth of the ejecta ( $M$  and  $V_e$ ) and on the chemical composition of the ejecta, since photoabsorption cuts off the lower energy side of the spectrum at  $E < 100 \text{ keV}$ . The value of the flux seen in the 200-400 keV band is in agreement with the predictions of the fiducial model. The overall shape of the spectrum (SPI+ISGRI data, see Fig.1) can be well fitted by other models having a ratio  $R = E_K/M \sim 10^{51} \text{ erg}/M_\odot$ , while the data place weaker constraints on  $E_K$  and  $M$  separately. This ratio corresponds to  $V_e \approx 2900 \text{ km s}^{-1}$ , i.e. slightly higher than the value derived from line fitting<sup>4</sup>. Allowing for systematic uncertainties and accounting for simplicity of the fitting functions we consider that the agreement is reasonable.

### 3.5. Conclusions and future work

The detection of key gamma-ray lines of radioactive cobalt  $^{56}\text{Co}$  provides solid proof of the interpretation of Type Ia supernova as a thermonuclear explosion of near-Chandrasekhar-mass WD. There is broad agreement between the observed fluxes and line broadening with the canonical model of the SNIa at the stage when the decay of  $^{56}\text{Co}$  dominates. More thorough comparison of the INTEGRAL data with the detailed models of emerging gamma-ray flux and optical data to differentiate between different explosion scenarios will be presented in subsequent publications.

### ACKNOWLEDGMENTS

Based on observations with INTEGRAL, an ESA project with instruments and science data centre funded by ESA member states (especially the PI countries: Denmark, France, Germany, Italy, Switzerland, Spain), Czech Republic and Poland, and with the participation of Russia and the USA. We are grateful to ESA INTE-

GRAL Team and Erik Kuulkers for prompt reaction to the SN2014J event. EC, RS, SG wish to thank Russian INTEGRAL advisory committee for allocating additional 1 Msec of time from a regular program to SN2014J observations. JI is supported by MINECO-FEDER and Generalitat de Catalunya grants. The SPI project has been completed under the responsibility and leadership of CNES/France. ISGRI has been realized by CEA with the support of CNES.

## 4. APPENDIX

### 4.1. SPI data analysis

The data analysis follows the scheme implemented in Churazov et al. (2005, 2011). For each detector, a linear relation between the energy and the channel number was assumed and calibrated (separately for each orbit), using the observed energies of lines at  $\sim 198, 438, 584, 882, 1764, 1779, 2223$  and  $2754 \text{ keV}$ . For our analysis we used a combination of single and pulse-shape-discriminator (PSD) events (see Vedrenne et al. 2003, for details) and treated them in the same way.

The flux from the supernova  $S(E)$  at energy  $E$  and the background rates in individual detectors  $B_i(E, t)$  were derived from a simple model of the observed rates  $D_i(E, t)$  in individual SPI detectors, where  $i$  is the detector number and  $t$  is the time of individual observations with a typical exposure of 2000 s:

$$D_i(E, t) \approx S(E) \times R_i(E, t) + B_i(E, t) + C_i(E), \quad (1)$$

where  $R_i(E, t)$  is the effective area for a given detector<sup>5</sup> as seen from the source position in a given observation and  $C_i(E)$  does not depend on time. The background rate is assumed to be linearly proportional to the Ge detectors saturated (i.e. above 8 MeV) event rate  $G_{\text{sat}}(t)$  averaged over all detectors, i.e.  $B_i(E, t) = \beta_i(E)G_{\text{sat}}(t)$ . The coefficients  $S(E)$ ,  $\beta_i(E)$  and  $C_i(E)$  are free parameters of the model and are obtained by minimizing  $\chi^2$  for the entire data set or for any (sufficiently large) subset of the data. A linear nature of the model allows for straightforward estimation of errors. The systematic uncertainties were evaluated by analyzing the SPI data with the method presented in Isern et al. (2013).

### 4.2. ISGRI data analysis

The ISGRI energy calibration use the procedure implemented in OSA 10.0<sup>6</sup>. The images in broad energy bands were reconstructed using standard mask/detector cross-correlation procedure, tuned to produce zero signal on the sky if the count rate across the detector matches the pattern expected from pure background, which was derived from the same dataset.

## REFERENCES

- Arnett, W. D. 1982, ApJ, 253, 785  
 Churazov, E., Sunyaev, R., Sazonov, S., Revnivtsev, M., & Varshalovich, D. 2005, MNRAS, 357, 1377  
 Churazov, E., Sazonov, S., Tsygankov, S., Sunyaev, R., & Varshalovich, D. 2011, MNRAS, 411, 1727  
 Churazov, E., Sunyaev, R., Grebenev, S., et al. 2014, The Astronomer's Telegram, 5992, 1  
 Dwarkadas, V. V., & Chevalier, R. A. 1998, ApJ, 497, 807  
 Gilfanov, M., & Bogdán, Á. 2010, Nature, 463, 924  
 Goobar, A., Johansson, J., Amanullah, R., et al. 2014, ApJ, 784, L12  
 Hillebrandt, W., & Niemeyer, J. C. 2000, ARA&A, 38, 191  
 Isern, J., Jean, P., Bravo, E., et al. 2013, A&A, 552, A97  
 Isern, J, et al. 2014, The Astronomer's Telegram, 6099, 1  
 Karachentsev, I. D., & Kashibadze, O. G. 2006, Astrophysics, 49, 3

<sup>4</sup> Note than a Gaussian may not be the best representation of the emergent shape of the lines.

<sup>5</sup> <https://heasarc.gsfc.nasa.gov/docs/integral/spi/pages/irf.html>

<sup>6</sup> <http://isdc.unige.ch/integral/analysis#Software>

- Kuulkers, E. 2014, *The Astronomer's Telegram*, 5835, 1
- Lebrun, F., Leray, J. P., Lavocat, P., et al. 2003, *A&A*, 411, L141
- Margutti, R., Parrent, J., Kamble, A., et al. 2014, arXiv:1405.1488
- Malone, C. M., Nonaka, A., Woosley, S. E., et al. 2014, *ApJ*, 782, 11
- Matz, S. M., Share, G. H., Leising, M. D., Chupp, E. L., & Vestrand, W. T. 1988, *Nature*, 331, 416
- Moll, R., Raskin, C., Kasen, D., & Woosley, S. E. 2014, *ApJ*, 785, 105
- Nadyozhin, D. K. 1994, *ApJS*, 92, 527
- Nomoto, K., Thielemann, F.-K., & Yokoi, K. 1984, *ApJ*, 286, 644
- Perlmutter, S., Aldering, G., Goldhaber, G., et al. 1999, *ApJ*, 517, 565
- Riess, A. G., Filippenko, A. V., Challis, P., et al. 1998, *AJ*, 116, 1009
- Röpke, F. K., Kromer, M., Seitzzahl, I. R., et al. 2012, *ApJ*, 750, L19
- Sazonov, S. Y., Lutovinov, A. A., & Krivonos, R. A. 2014, *Astronomy Letters*, 40, 65
- Sunyaev, R., Kaniovsky, A., Efremov, V., et al. 1987, *Nature*, 330, 227
- Sunyaev, R. A., Kaniovskii, A. S., Efremov, V. V., et al. 1990, *Soviet Astronomy Letters*, 16, 171
- The, L.-S., & Burrows, A. 2014, *ApJ*, 786, 141
- Ubertini, P., Lebrun, F., Di Cocco, G., et al. 2003, *A&A*, 411, L131
- Winkler, C., Courvoisier, T. J.-L., Di Cocco, G., et al. 2003, *A&A*, 411, L1
- Woosley, S. E., & Weaver, T. A. 1986, *ARA&A*, 24, 205
- Woosley, S. E., Kasen, D., Blinnikov, S., & Sorokina, E. 2007, *ApJ*, 662, 487
- Vedrenne, G., Roques, J.-P., Schönfelder, V., et al. 2003, *A&A*, 411, L63
- Zheng, W., Shivvers, I., Filippenko, A. V., et al. 2014, *ApJ*, 783, L24